Supplementary Material

Photocatalytic performance of carbon-containing Cu-Mo-based catalysts under sunlight illumination

Paula Muñoz-Flores [a,b,*], Po S. Poon [a], Catherine Sepulveda [c], Conchi O. Ania [d,*], Juan Matos [e,*]

[a] Unidad de Desarrollo Tecnológico (UDT), Universidad de Concepción, Barrio Universitario s/n, Concepción, Chile.

[b] Departamento de Ingeniería Química, Facultad de Ingeniería, Universidad de Concepción, Barrio Universitario s/n, Concepción, Chile.

[c] Facultad de Ciencias Químicas, Universidad de Concepción, Casilla 160C, Chile.

[d] CEMHTI, CNRS (UPR 3079), Université d'Orléans, 45071 Orléans, France.

[e] Instituto de Ciencias Químicas Aplicadas, Facultad de Ingeniería, Universidad Autónoma de Chile, 8900000 Santiago, Chile.

*Corresponding authors E-mails: paulamunozf@udec.cl (P. Muñoz-Flores); conchi.ania@cnrs-orleans.fr (C.O. Ania); juan.matos@uautonoma.cl (J. Matos)

Phone: +56 9 9379 8340

Table S1. Yields of synthesis and stoichiometric expressions describing the thermal degradation of furfural, Cu- and Mo-salts.

Step	Sample [a]	Average yield (%)	Global yield (%) [b]
1st	Cu4	30 ± 1	30 ± 1
2nd	Cu4-350-O_2	76 ± 3	23 ± 4
2nd	Cu4-550-O_2	67 ± 8	20 ± 9
2nd	Cu4-800-N_2	77 ± 4	23 ± 5
1st	Mo4	73 ± 3	73 ± 3
2nd	Mo4-350-O_2	73 ± 6	53 ± 9
2nd	Mo4-550-O_2	71 ± 5	52 ± 8
2nd	Mo4-800-N_2	64 ± 2	47 ± 5
1st	Cu4Mo4	69 ± 3	69 ± 3
2nd	Cu4Mo4-350-O_2	80 ± 5	55 ± 8
2nd	Cu4Mo4-550-O_2	76 ± 3	52 ± 6
2nd	Cu4Mo4-800-N_2	75 ± 2	52 ± 5

[a] The nominal weight expected of solid carbon C formed from furfural thermal degradation is ca. 0.312 g,

$$C_5H_4O_2 \rightarrow 5C + 2H_2O \quad (1), [1].$$

The nominal weight expected of CuO from $Cu(O_2C_5H_7)_2$ is ca. 0.152 g,

$$Cu(O_2C_5H_7)_2 + 12O_2 \rightarrow CuO + 7H_2O + 10CO_2 \quad (2), [2].$$

The nominal weight expected for MoO_3 from $(NH_4)_6Mo_7O_{24}\cdot 4H_2O$ is ca. 0.408 g,

$$(NH_4)_6Mo_7O_{24}\cdot 4H_2O \rightarrow 7MoO_3 + 7H_2O + 6NH_3 \quad (3), [3].$$

Thus, a total nominal weight of ca. 0.464 g is expected for the synthesis of the Cu4 catalyst. Similarly, the total nominal weight expected for Mo4 and Cu4Mo4 catalysts are ca. 0.720 g, and 0.872 g, respectively.

[b] Global yield estimated from the product between the average yield at first-step and second-step and then divided by 100.

[1] J. Matos, P. Atienzar, H. García, J.C.J. Hernández-Garrido. Nanocrystalline carbon–TiO_2 hybrid hollow spheres as possible electrodes for solar cells. Carbon. 53 (2013) 169 –181.
[2] R.S. Mann, K.C. Khulbe. ESR study of MoO_3 obtained from thermal decomposition of ammonium molybdate. Bull. Chem. Soc. Japan. 48 (1975) 1021-1023.
[3] Q. Jin, M. Fujishima, A. Iwaszuk, M. Nolan, H. Tada. Loading effect in copper (II) oxide cluster-surface-modified titanium (IV) oxide on visible- and UV-light activities. J. Phys. Chem. C. 117 (2013) 23848-23857.

Table S2. Summary of the proximate analysis of the prepared catalysts.

Catalysts	Moisture (wt. %)	Inorganic Content (wt. %)	Carbon Content (wt. %)
Cu4	1.1 ± 0.1	45.2 ± 0.9	53.7 ± 0.7
Cu4-350-O_2	0.26 ± 0.05	91.0 ± 0.7	9.1 ± 0.2
Cu4-550-O_2	0.40 ± 0.08	97.7 ± 0.3	1.9 ± 0.4
Cu4-800-N_2	1.6 ± 0.1	78.1 ± 0.5	20.3 ± 0.6
Mo4	0.70 ± 0.03	74.3 ± 0.1	25.0 ± 0.6
Mo4-350-O_2	0.90 ± 0.03	95.1 ± 0.1	4.0 ± 0.1
Mo4-550-O_2	0.64 ± 0.02	98.7 ± 0.5	0.66 ± 0.08
Mo4-800-N_2	0.40 ± 0.02	91.3 ± 0.7	8.3 ± 0.5
Cu4Mo4	0.90 ± 0.07	83.4 ± 0.2	15.7 ± 0.2
Cu4Mo4-350-O_2	0.60 ± 0.01	96.4 ± 0.9	3.0 ± 0.2
Cu4Mo4-550-O_2	0.34 ± 0.05	99.3 ± 0.8	0.36 ± 0.05
Cu4Mo4-800-N_2	0.80 ± 0.02	95.3 ± 0.7	3.9 ± 0.3

Table S3. Summary of kinetic models for the analysis of the kinetic data of Y5 adsorption.

Kinetic model	Equation
Pseudo-first-order	$\log(n_{eq} - n_{ads}) = \log(n_{eq}) - (k_1/2.303)\ t$
Pseudo-second-order	$(1/n_{eq} - n_{ads}) = (1/n_{eq}) + k_2\ t$
Intraparticle diffusion	$n_{ads\text{-}t} = C + k_p\ t^{1/2}$

The pseudo-first-order model showed in Eq. (1), where k_1 is the pseudo-first-order rate constant (min^{-1}) for the adsorption, n_{ads} the amount of tallow 5 (Y5) adsorbed (in μmol), at time t (min) and n_{eq} is the amount adsorbed at equilibrium (in μmol).

$$dn_{ads}/dt = k_1(n_{eq} - n_{ads}) \quad (1)$$

The integration of Eq. (1) at the initial conditions ($n_{ads} = 0$ at $t = 0$) yields the Eq. (2):

$$\log(n_{eq} - n_{ads}) = \log(n_{eq}) - (k_1/2.303).t \quad (2)$$

In addition, a pseudo-second-order equation may be expressed by Eq. (3):

$$dn_{ads}/dt = k_2(n_{eq} - n_{ads})^2 \quad (3)$$

Where k_2 is the pseudo-second-order rate constant ($\mu mol^{-1}.min^{-1}$) for the adsorption. Applying the initial conditions, Eq. (3) can be integrated to obtain Eq. (4):

$$(1/n_{eq} - n_{ads}) = (1/n_{eq}) + k_2.t \quad (4)$$

The influence of the intraparticle diffusion phenomena upon the adsorption capacity of Y5 was verified keeping in mind that the fractional approach to equilibrium change is done according to a function of $(D_t/r^2)^{1/2}$, where r is the radius of adsorbent particle and D is the effective diffusivity of solute within the particle. The initial rate according to the intraparticle diffusion model (IPD) is obtained from the liner regression of the curve $n_{ads\text{-}t} = f(t^{1/2})$, expressed by the Eq. (5) where k_p is the IPD rate constant ($\mu mol\ min^{-0.5}$), and C is a constant (μmol) attributed to the extension of the boundary layer thickness.

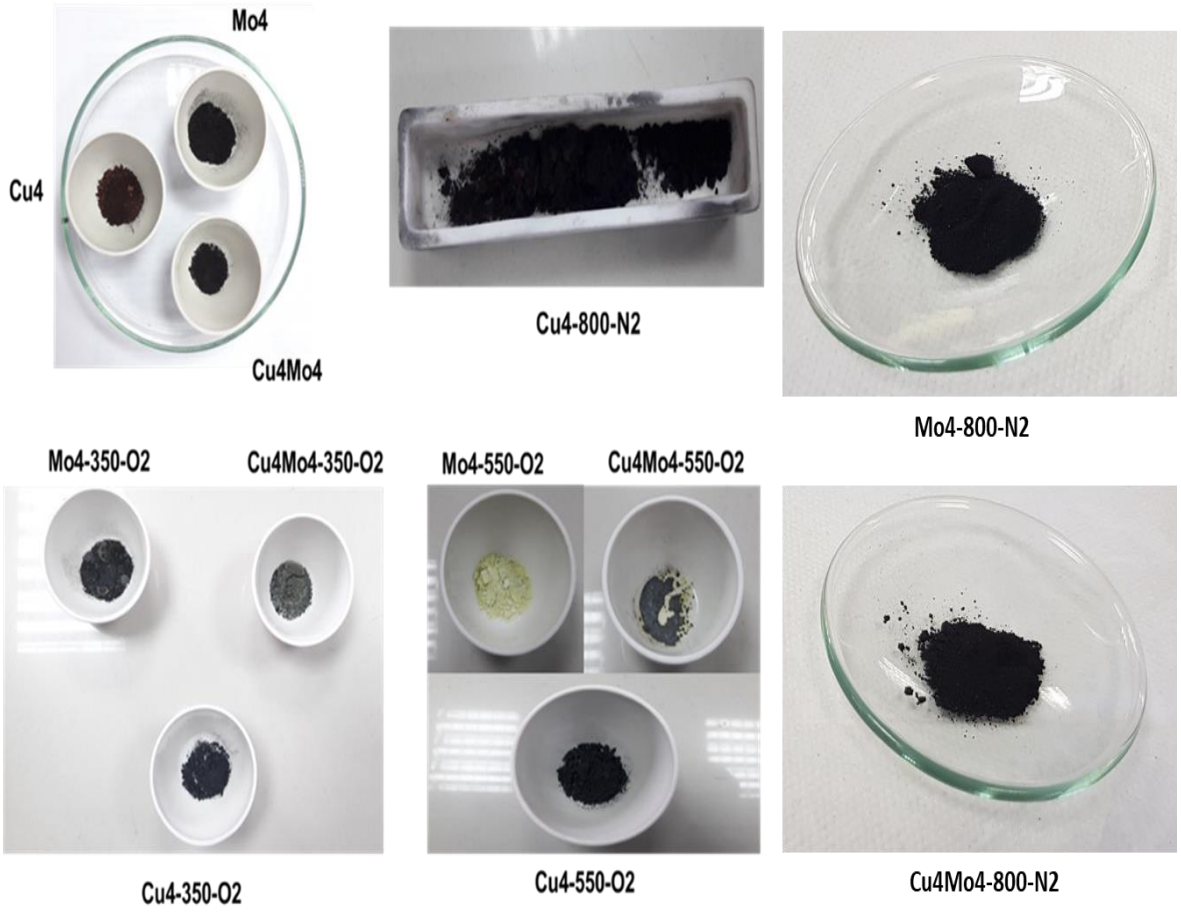

Figure S1. Images of the Cu-, Mo-, and CuMo-based photocatalysts prepared.

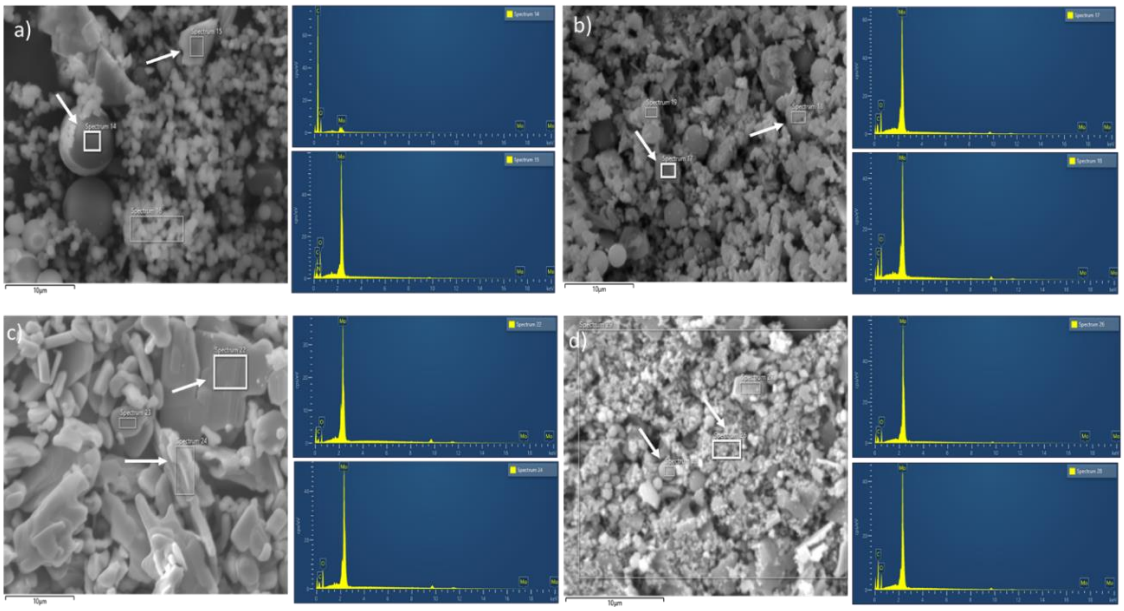

Figure S2. Composition of SEM-EDS analysis of Mo-based catalysts. a) Mo4; b) Mo4-350-O_2; c) Mo4-550-O_2; d) Mo4-800-N_2.

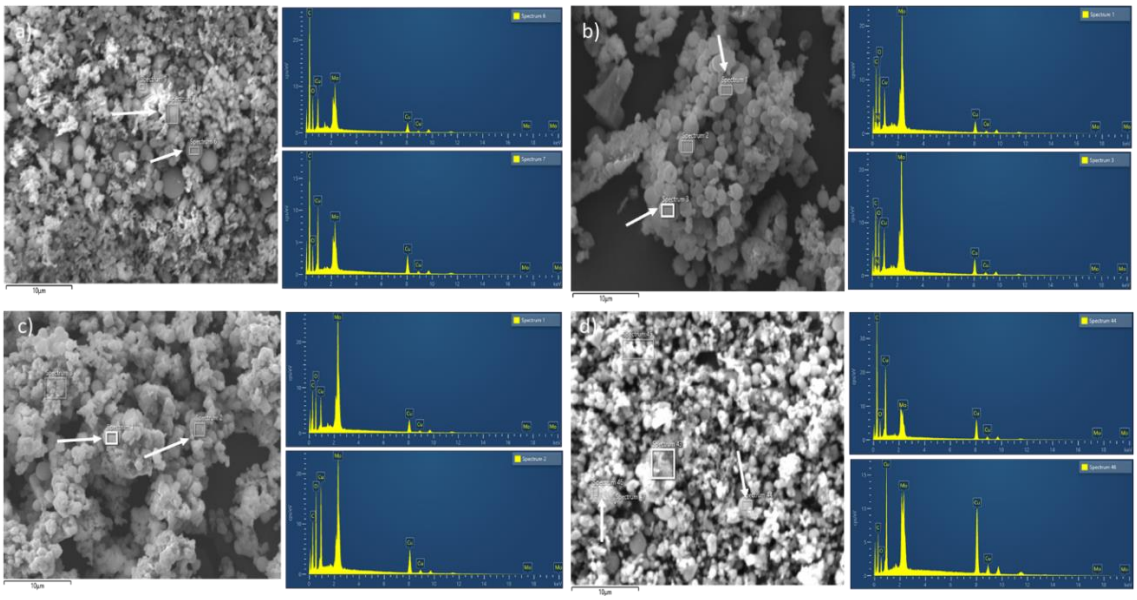

Figure S3. Composition of SEM-EDS analysis of CuMo-based catalysts. a) Cu4Mo4; b) Cu4Mo4-350-O_2; c) Cu4Mo4-550-O_2; d) Cu4Mo4-800-N_2.

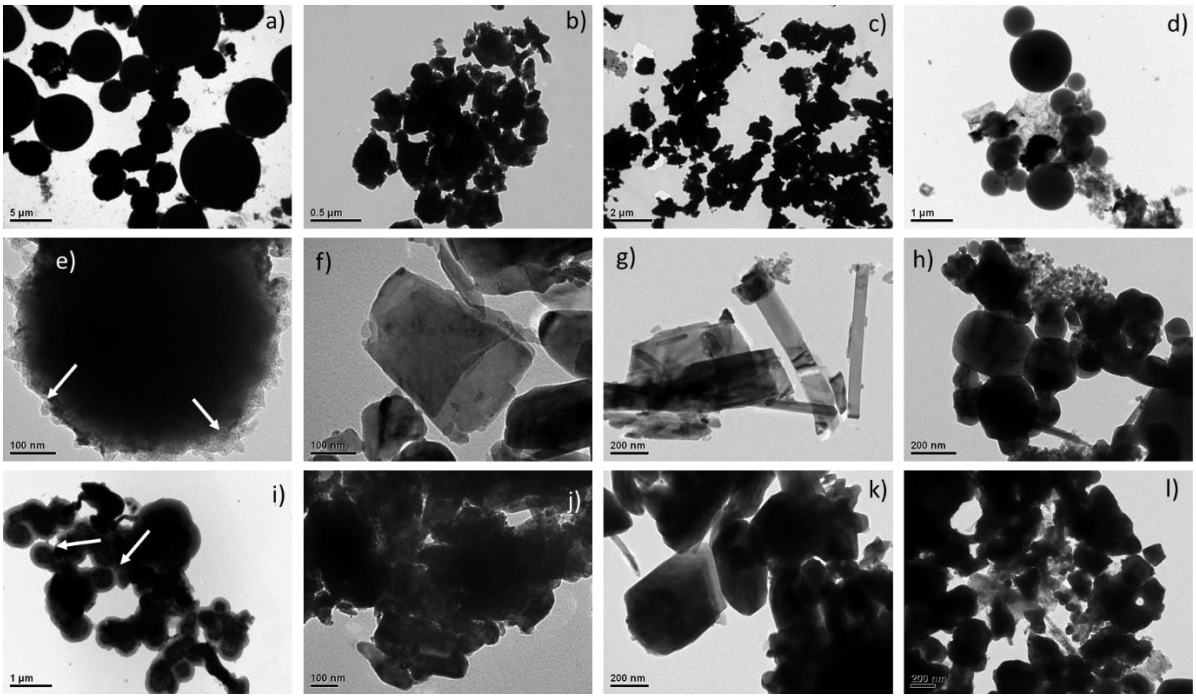

Figure S4. Transmission electron microscopy images. a) Cu4; b) Cu4-350-O_2; c) Cu4-550-O_2; d) Cu4-800-N_2; e) Mo4; f) Mo4-350-O_2; g) Mo4-550-O_2; h) Mo4-800-N_2; i) Cu4Mo4; j) Cu4Mo4-350-O_2; k) Cu4Mo4-550-O_2; l) Cu4Mo4-800-N_2.

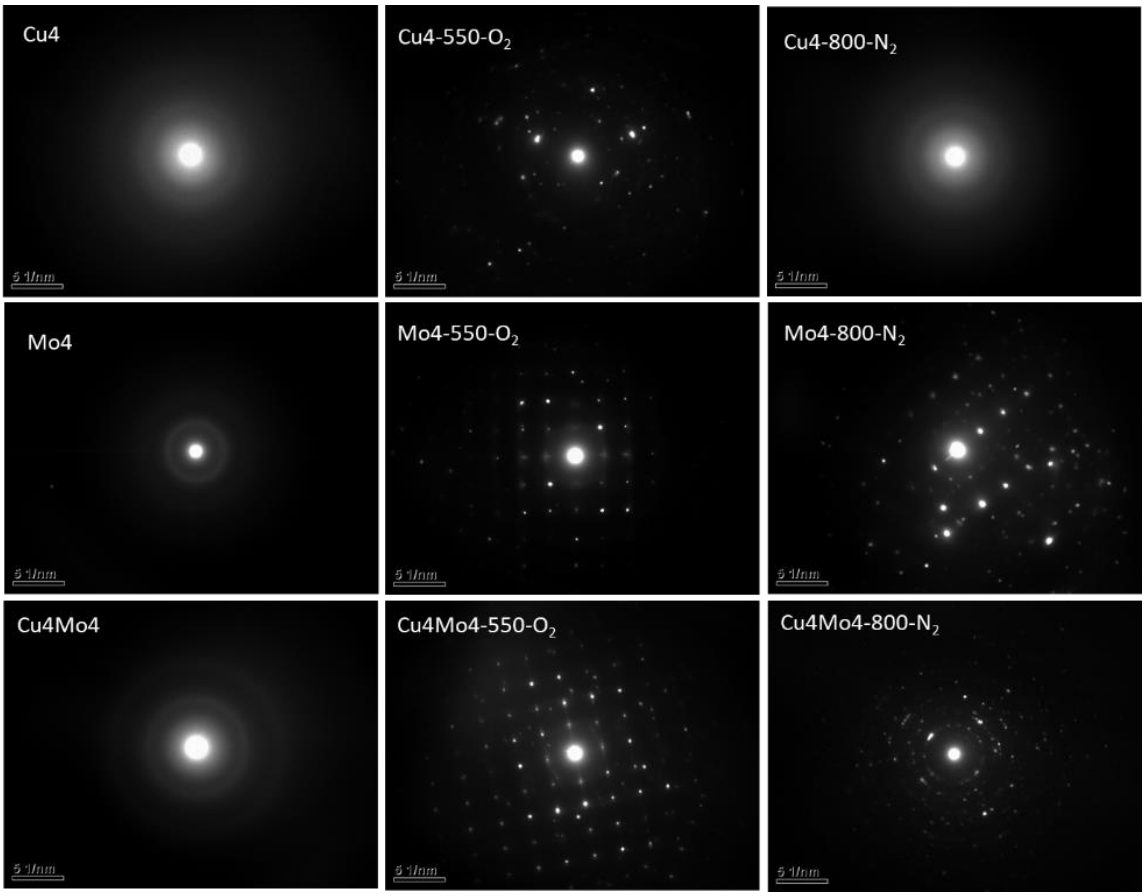

Figure S5. Selected ED patterns of catalysts.

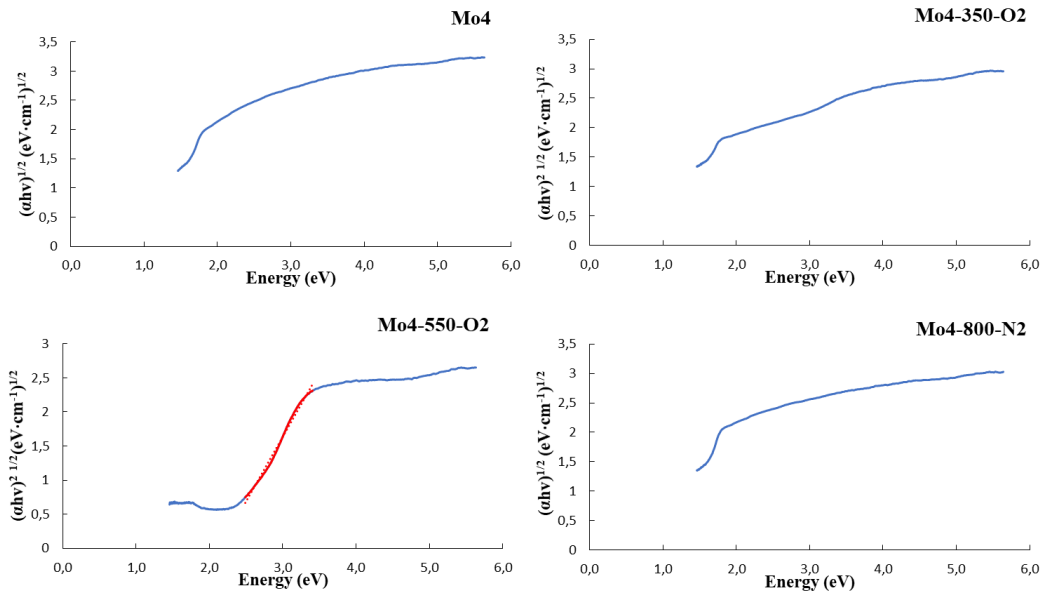

Figure S6. Tauc representation from the Kubelka–Munk function of Mo-based materials.

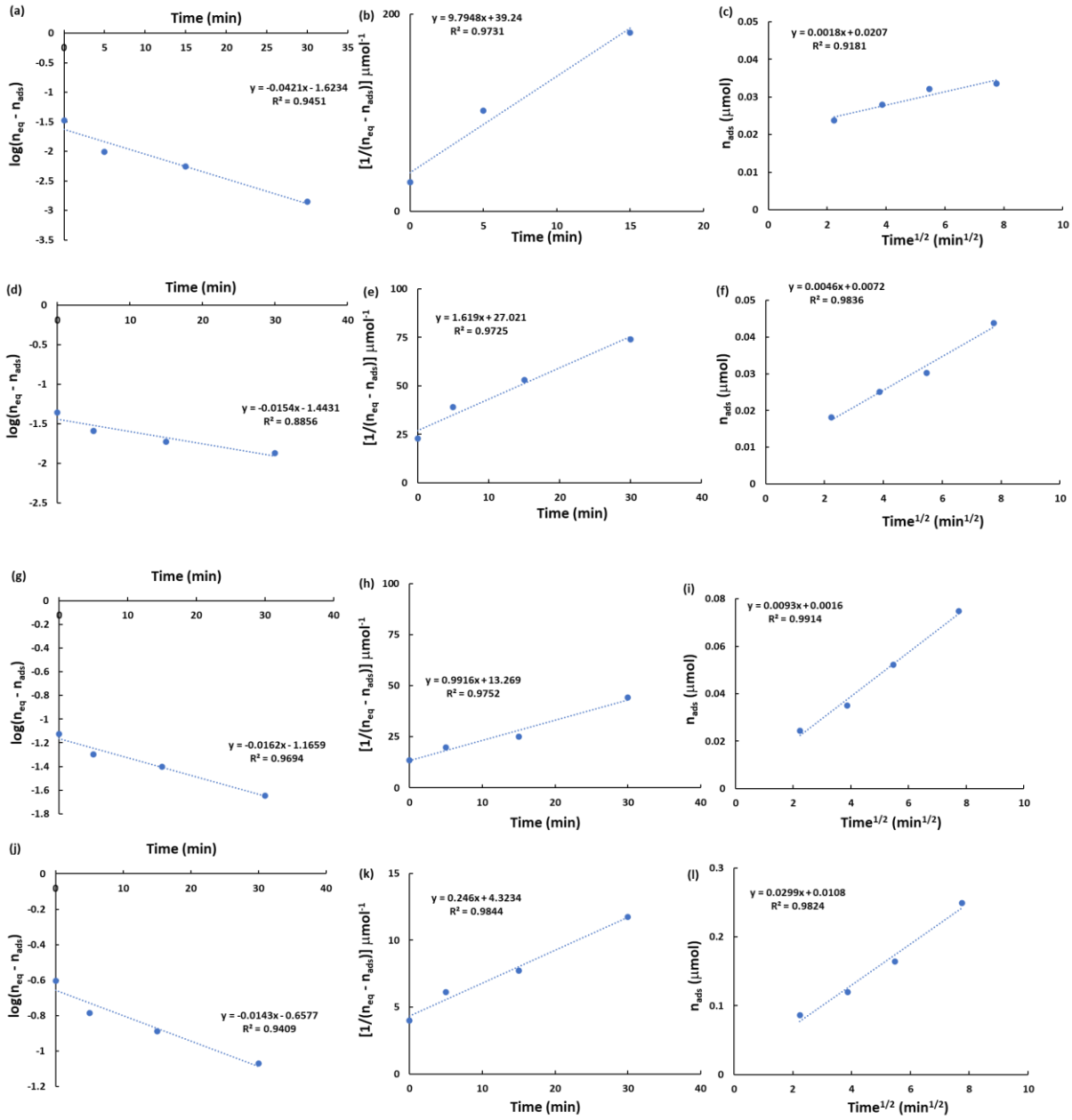

Figure S7. Fitting of the experimental kinetic data for Y5 adsorption on the Cu-based photocatalysts, using different models: Left: Pseudo first-order; Middle: Pseudo second-order; Right: Intraparticle diffusion model. (a,b,c): Cu4; (d,e,f): Cu4-350-O_2; (g,h,i): Cu4-550-O_2; (j,k,l): Cu4-800-N_2.

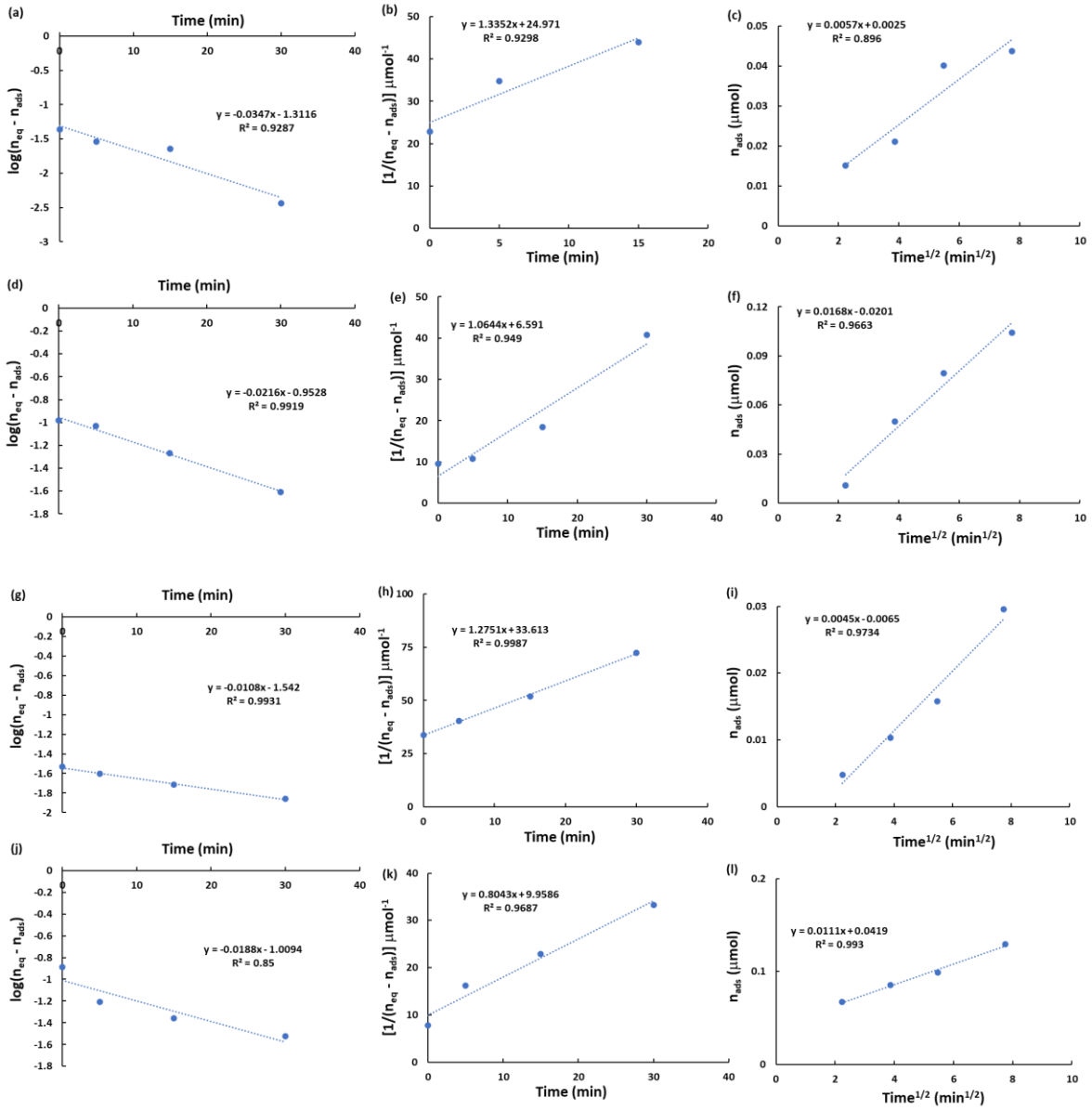

Figure S8. Fitting of the experimental kinetic data for Y5 adsorption on the Mo-based photocatalysts, using different models: Pseudo first-order; Middle: Pseudo second-order; Right: Intraparticle diffusion model. (a,b,c): Mo4; (d,e,f): Mo4-350-O_2; (g,h,i): Mo4-550-O_2; (j,k,l): Mo4-800-N_2.

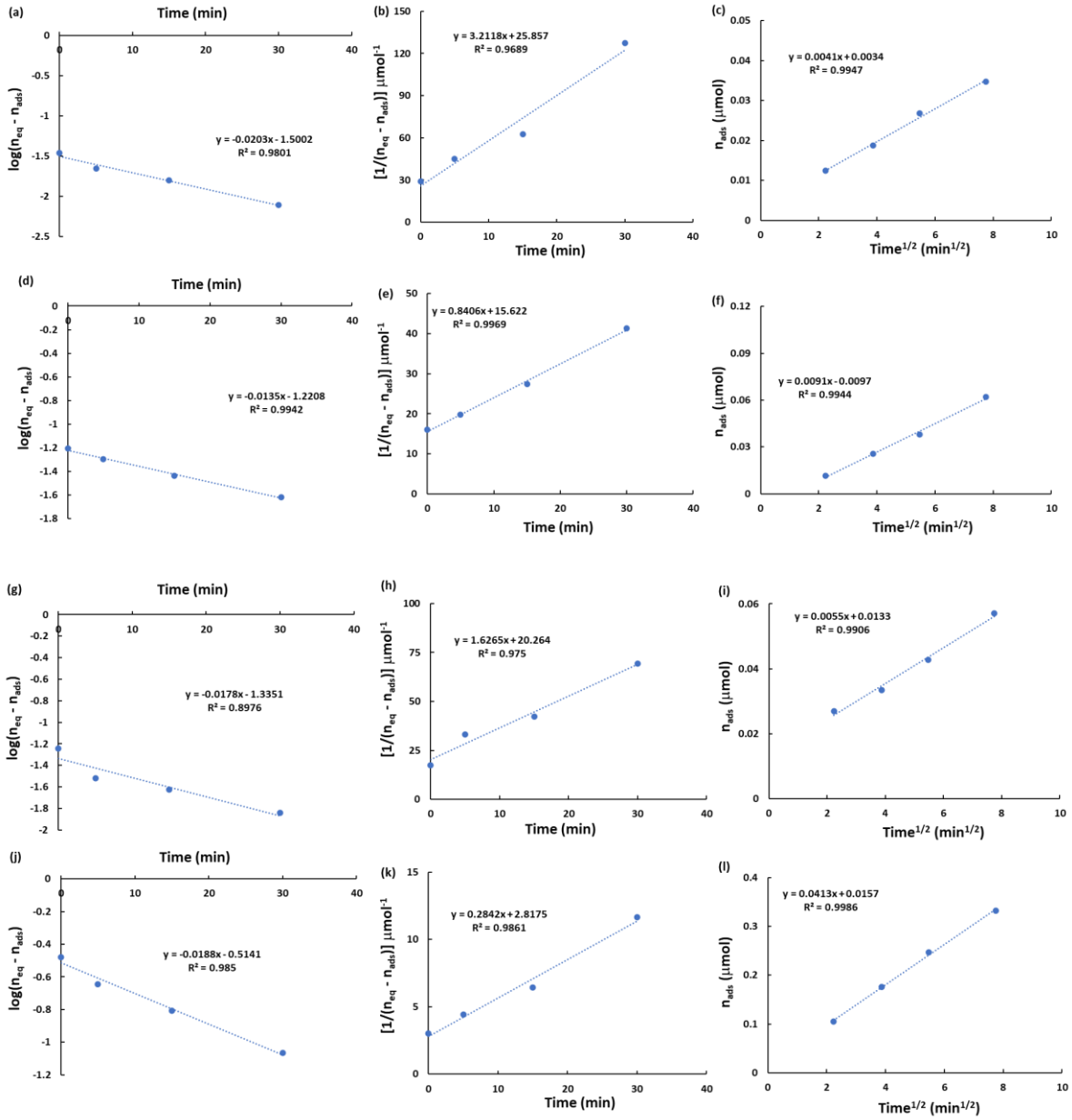

Figure S9. Fitting of the experimental kinetic data for Y5 adsorption on the CuMo-based photocatalysts, using different models: Left: Pseudo first-order; Middle: Pseudo second-order; Right: Intraparticle diffusion model. (a,b,c): Cu4Mo4; (d,e,f): Cu4Mo4-350-O_2; (g,h,i): Cu4Mo4-550-O_2; (j,k,l): Cu4Mo4-800-N_2.

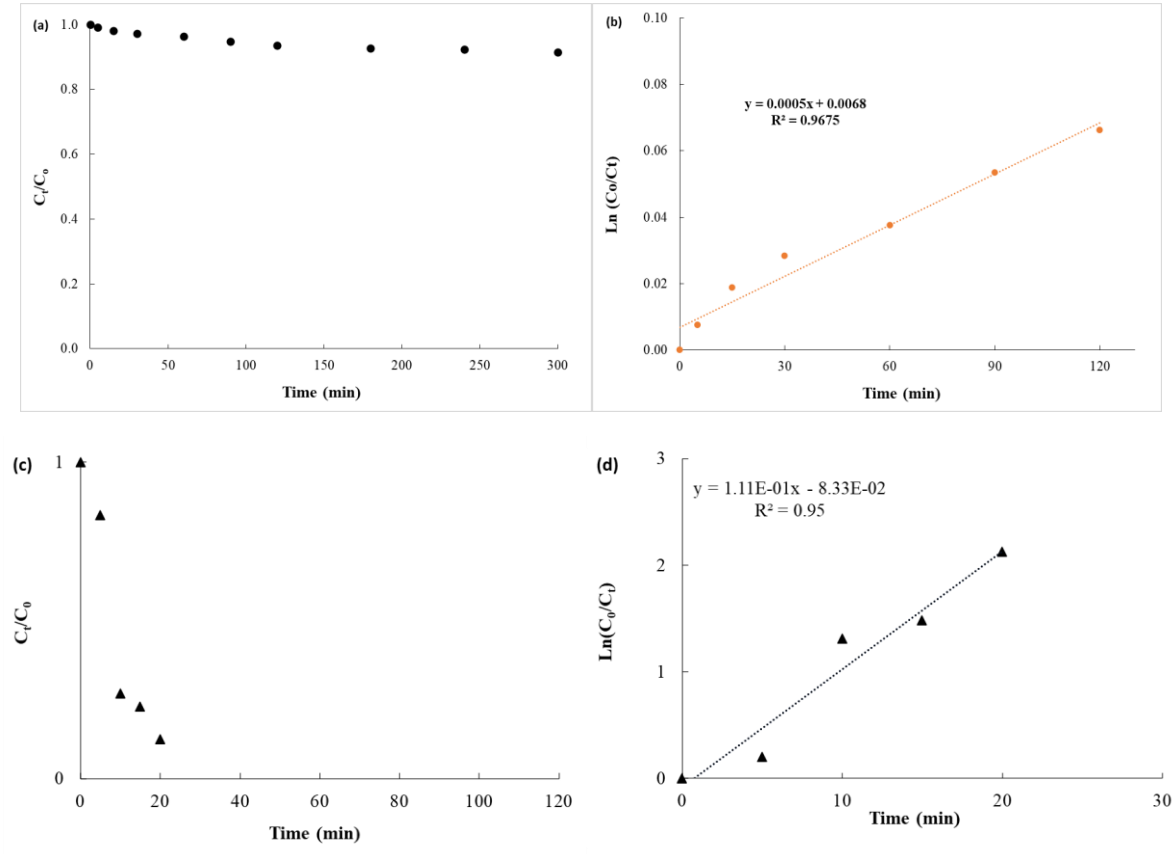

Figure S10. (a) Kinetics of Y5 disappearance upon direct photolysis. (b) Linear regression of the kinetics data from **Figure S10a**. (c) Kinetics of Y5 disappearance on irradiated TiO_2-P25. (d) Linear regression of the kinetics data from **Figure S10c**. Initial concentration: 5ppm.

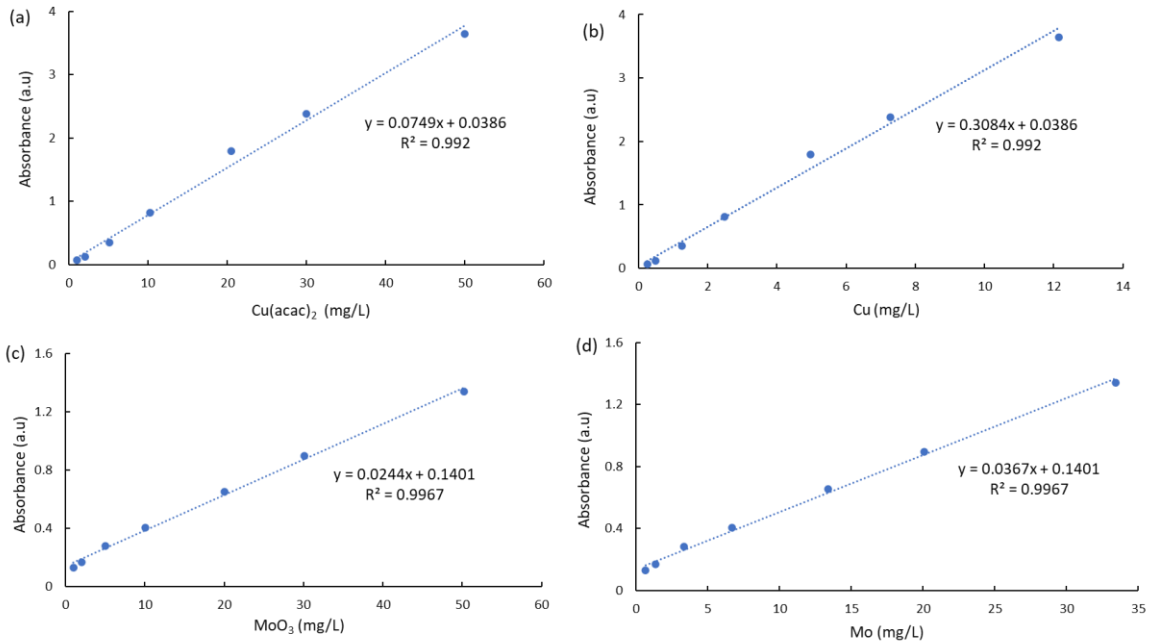

Figure S11. Calibration curves for the determination of copper (290 nm) and molybdenum (208 nm) ions in the leaching tests: (a) $Cu(acac)_2$; (b) expressed as equivalent Cu(II) in $Cu(acac)_2$; (c): MoO_3; (d) expressed as equivalent Mo(III) in MoO_3.